Spectroscopy 18 (2004) 587–596
IOS Press

Development and AFM study of porous scaffolds for wound healing applications

T.A. Doneva [a,*], H.B. Yin [a], P. Stephens [b], W.R. Bowen [a] and D.W. Thomas [b]

[a] *Centre for Complex Fluids Processing, School of Engineering, University of Wales, Swansea, Singleton Park, Swansea, SA2 8PP, UK*

[b] *Wound Biology Group, Dept. Oral Surgery, Medicine & Pathology, University of Wales College of Medicine, Cardiff, CF14 4XY, UK*

Abstract. An engineering approach to the development of biomaterials for promotion of wound healing emphasises the importance of a well-controlled architecture and concentrates on optimisation of morphology and surface chemistry to stimulate guidance of the cells within the wound environment. A series of three-dimensional porous scaffolds with 80–90% bulk porosity and fully interconnected macropores were prepared from two biodegradable materials – cellulose acetate (CA) and poly (lactic-co-glycolic acid) (PLGA) through the phase inversion mechanism of formation. Surface morphology of obtained scaffolds was determined using atomic force microscopy (AFM) in conjunction with optical microscopy. Scanning Electron Microscopy (SEM) was applied to characterise scaffolds bulk morphology. Biocompatibility and biofunctionality of the prepared materials were assessed through a systematic study of cell/material interactions using atomic force microscopy (AFM) methodologies together with *in vitro* cellular assays. Preliminary data with human fibroblasts demonstrated a positive influence of both scaffolds on cellular attachment and growth. The adhesion of cells on both biomaterials were quantified by AFM force measurements in conjunction with a cell probe technique since, for the first time, a fibroblast probe has been successfully developed and optimal conditions of immobilisation of the cells on the AFM cantilever have been experimentally determined.

Keywords: Biomaterials, porous polymer scaffolds, cell/material interactions, wound healing, AFM

1. Introduction

The ability of synthetic and biological polymers to support and guide invasion of cells from surrounding tissue is a key parameter for tissue engineering (TE) and wound healing.

Most porous scaffolds have been prepared from aliphatic polyester such as poly(lactic acid) (PLA), poly(glycolic acid) (PGA) and their copolymer of poly(DL-lactic-co-glycolic acid) [1]. Pore size, porosity, interconnectivity between pores and surface area are generally considered to affect cell attachment or cell growth [2] but the evidence is still equivocal. A fundamental understanding of the mechanisms of biomaterials-induced modulation of wound repair process requires interdisciplinary approaches that relate physicochemical and morphological properties of scaffolds to bio-surface interactions at the macromolecule and cell level. AFM is a novel concept that integrates engineering and life sciences into the field of nanoscience and nanotechnology in order to generate new synergies in research. As an imaging device AFM provides high-resolution images of biological structures such as DNA, proteins [3], living

*Corresponding author: T.A. Doneva, Centre for Complex Fluids Processing, School of Engineering, University of Wales, Swansea, Singleton Park, Swansea, SA2 8PP, UK. Tel.: +44 (0) 1792 205678, ext. 4093; Fax: +44 (0) 1792 295701; E-mail: t.a.doneva@swansea.ac.uk.

cells [4] and biological processes [5]. As a force sensor, AFM in conjunction with colloid and cell probe techniques allows direct quantification of materials' surface properties as well as cellular interactions with surfaces of interest [6,7].

Importantly, the performance of polymer porous scaffolds for medical applications is controlled by their biocompatibility and biofunctionality [8].

In the present study, three-dimensional porous scaffolds of well-controlled morphology and chemistry were prepared from the synthetic, cost-effective polymer cellulose acetate (CA) and PLGA as a reference material using the phase inversion mechanism of formation. Both the materials have previously not been systematically investigated in the field of dermal wound healing. Their biocompatibility and cytotoxity were evaluated with a cell proliferation assay utilising human fibroblasts. The biofunctionality of the obtained biomaterials was assessed through a cell/material attachment assay and fibroblast adhesion on the scaffold surfaces was directly quantified using AFM force measurements in conjunction with a recently developed, novel mammalian cell probe.

2. Materials and methods

2.1. Materials

Poly(D,L-lactic-co-glycolic acid) (PLGA 75/25) was kindly provided by Particulate Fluids Processing Centre, Melbourne University, Australia. Cellulose acetate (CA-394-60S) was purchased from Eastman chemical company. PVP (polyvinylpyrrolidone) (M_w 55,000), dioxane, acetone, and dimethylformide (DMF) were purchased from Aldrich. All chemicals were used without further purification. All cell culture reagents were purchased from Life Technologies, UK.

2.2. Preparation of porous scaffolds

Wet phase inversion method was applied for both scaffolds. PLGA or PLGA/PVP blend was dissolved in dioxane to form a uniform solution. The casting solutions were left for 1 day to release bubbles. They were then cast onto a glass plate by doctor blade at a thickness of 500 μm and evaporated in air for 2.5 minutes. The wet films were put into ethanol or a mixture of dioxane/ethanol nonsolvent bath for 30 minutes and were subsequently washed thoroughly with deionized water to remove residual solvent.

Cellulose acetate was dissolved in mixture of DMF/acetone (DMF : acetone $= 2 : 3$) to form a uniform solution at concentration of 6 wt%. The solution was cast on a glass plate at a thickness of 500 μm, exposed in air for 2 minutes, and immersed in a coagulation bath of deionized water to form a thin film. All the materials were then dried in vacuum for 2 days and kept in desiccators before use.

2.3. Characterisation studies

2.3.1. Surface and bulk morphology

Surface morphology of scaffolds was determined with optical microscopy (Singer Instruments, UK) and atomic force microscopy (Autoprobe CP-100, Park Scientific Instruments). Scanning electron microscopy (Philips XL30 CP SEM) was used to characterise scaffolds bulk morphology. All samples were soaked in deionized water for 24 hours before measurements.

2.3.2. Hydration and bulk porosity of scaffolds

The water uptake capacity of scaffolds was described as the percentage of adsorbed water of a scaffold, which is determined by hydration of scaffolds in deionised water at room temperature for 24 hours to reach the equilibrium stages expressed [9]. The bulk porosity of scaffolds was calculated according to previous studies ($\varepsilon_B\% = (1 - (\rho^* - \rho)) \times 100\%$, ρ^* – apparent density of the scaffolds, ρ – density of the solid polymers, 1.3 g/cm^3 for PLGA and 0.4 g/cm^3 for CA-398-10) [10].

2.4. Biocompatibility and biofunctionality of PLGA and CA scaffolds

The evaluation of the *in vitro* cytotoxicity of a biomaterial is the initial step on a biocompatibility study, and is usually performed using immortalised cell lines [11]. HCA2 immortalised foreskin fibroblasts [12], a kind gift from Professor David Kipling (Dept. Pathology, University of Wales College of Medicine), were used to study the cell/scaffolds interactions.

2.4.1. Cell/biomaterial adhesion

The adhesion of single fibroblast cells on both biomaterials was quantified by AFM force measurements in conjunction with a novel, mammalian cell probe technique. HCA2 cells of average size 15 μm were attached to the AFM cantilever (Fig. 1) by 20% glue (poly[2-hydroxyethyl-methacrylate]) dissolved in dimethyl sulphoxide (DMSO). This polymer/solvent combination demonstrated the best results: no toxicity to fibroblasts (assessed by 3-day growth assay) and strong covalent bonds between the cell and the cantilever surface. All force measurements were performed in PBS solution of pH 7.3, at low loading force using an Autoprobe CP-100 (Park Scientific Instruments) and V-shaped AFM tipples cantilevers with a specified spring constant of 0.4 N/m. Both scaffolds were soaked in PBS for 12 h before the experiment. Two sets of time dependant adhesion assays were carried out in order to define the different stages of the initial cell/material attachment. (1) Short time adhesion study: Fibroblast probe was brought in contact with PLGA, CA and poly-L (lysine) modified chamber slide used as a control. The adhesion force was estimated from the force/distance retraction curve after the first contact, 5 min contact and 10 min contact of the cell with the surface of all the materials. (2) Dynamic long time adhesion study: Adhesion between fibroblast cell and CA was quantified from the force/distance retraction curve after long time contact (1 h, 2 h, respectively) in order to assess the effect of cell spreading and synthesis

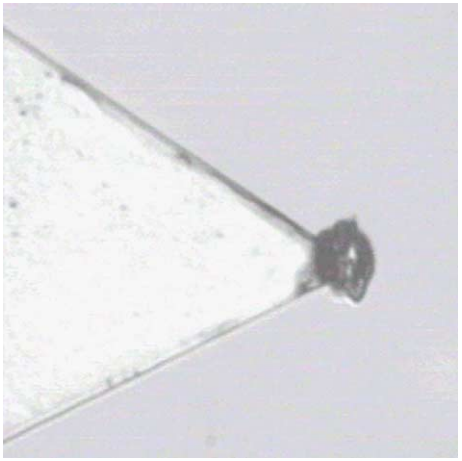

Fig. 1. HCA2 fibroblast cell probe attached on the AFM cantilever.

of ECM components on cell/material attachment. The contact duration between cell and material surface was acquired by adjusting the speed of piezo extension.

2.4.2. Cell/biomaterial proliferation (MTT assay)

Materials were prepared in 13 mm $\times$ 10 mm sections, sterilised in 70% ethanol and attached to the base of individual wells of an 8-well chamber slide (Beckton Dickinson Labware, Franklin Lakes, USA) using 12% (v/v) poly[2-hydroxyethyl-methacrylate] (Aldrich Chem. Co., UK) so as to prevent cells adhering underneath the material. Wells with adhesive and without materials were used as control. The 3-2,5-diphenyltetrazolium bromide (MTT) dye-reduction assay was performed on HCA2 fibroblasts recovered from culture by trypsinisation and seeded onto the materials at a cell density of 5×10^4 cells/well in 500 μl of F-SCM. After 72 hours 100 μl of 3-2,5 MTT (5 mg/ml; Sigma, Poole, UK) was added to each well and the plates incubated for 4 hours at 37°C. Media and MTT was then removed and 300 μl of extraction buffer (10% (w/v) sodium dodecyl sulphate (SDS)/0.5 M dimethylformamide; Sigma) was then added to each chamber and the plates incubated overnight at 37°C. Multiple 100 μl aliquots of extraction buffer containing solublised formazan were then added to wells of a 96-well microtitre plate (Greiner Bio-one Ltd., Stonehouse, UK) and the absorbance of each well was then assessed using a Dynex MRX spectrophotometer (Dynex Technologies, Billinghurst, UK) equipped with a 550 nm filter. Statistical analysis was performed using Student's 't' test.

3. Results

3.1. Properties of the fabricated scaffolds

Phase separation provides the flexibility to tailor pore size, porosity by adjusting process parameters. Table 1 shows the compositions, casting conditions and the subsequent surface properties of the prepared PLGA scaffolds. By evaporating solvent chloroform, PN scaffolds formed from the PLGA/Chloroform system have a very tight surface with a few of nanoscale pores. For the PLGA/dioxane/water systems, three kinds of porous PLGA scaffolds were formed. PLGA1 prepared in pure ethanol nonsolvent had the smallest average pore diameter of 1.0 μm, lowest porosity and broad pore size distribution. The addition of solvent dioxane into ethanol as a nonsolvent bath resulted in larger pores and higher porosity of PLGA2. Worthy to note, the addition of a small amount of PVP (0.2 wt%) gave a remarkable increase in porosity, almost more than a factor of 4 for PLGA3. Both the surface and the internal cross-section of the PLGA3 scaffold present a highly porous and uniform structure (Fig. 2). In contrast to PLGA scaffolds, a CA1 thin scaffold has a macroporous network structure (Fig. 3a). Clusters of small pores at average size of 19 ± 4 μm were formed in larger netlike pores with an average diameter of 108 ± 23 μm. However, the porous structure of the surface and internal pore wall of the polymeric struts with smaller pores were observed, as shown in Figs 3b and 3c. PLGA3 and CA1 scaffolds showed high water uptake capacity of 590% and 300%, respectively. As a result, there was a big difference between the bulk porosity of dry scaffolds and the wet scaffolds at the equilibrium stages. As the scaffolds were used in wet conditions, the wet bulk porosity should be considered. The wet bulk porosity of 90% for PLGA3 and of 80% for CA1 indicated highly porous bulk structure of both scaffolds.

The PLGA3 and CA1 scaffolds demonstrated the most promising properties and were further investigated for their biocompatibility and biofunctionality.

Table 1
Composition and surface morphology of PLGA scaffolds*

Type	Composition (g)	Non-solvent	D (μm)	ε_{sur} %
PN	PLGA/chloroform (8.5/91.5)	air	0.03±0.02	0.7
PLGA1	PLGA/dioxane (8.5/91.5)	ethanol	1.0±0.4	3.9
PLGA2	PLGA / dioxane (8.5/91.5)	ethanol/dioxane (4 : 1)	3.7±1.7	14.4
PLGA3	PLGA/dioxane/PVP (8.3/91.5/0.2)	ethanol/dioxane (4 : 1)	5.5±0.6	64.2

*Average pore diameter D and surface porosity were measured by AFM.

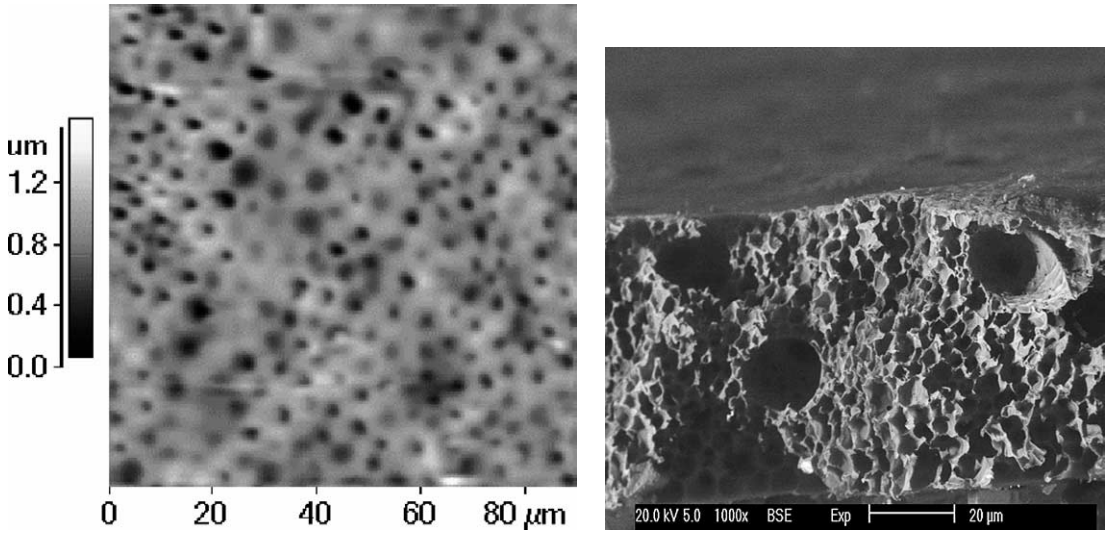

(a) (b)

Fig. 2. (a) AFM image of the surface of PLGA 3 scaffold; (b) SEM image of the internal cross-section of PLGA 3 scaffold.

3.2. Quantification of cell adhesion on the biomaterials

The initial overall fibroblast adhesion on both scaffolds is much lower compared to the cell adhesion on the control surface (Table 2). Cells adhered preferentially on the PLGA3 than CA1. The adhesion on the control surface and on PLGA3 did not change a lot after 10-min contact with the cell (factor 1.5 for the glass and 1.2 for PLGA3). In contrast, the adhesion on CA1 increased significantly after 10-min contact with the cell (factor 5). Further prolongation of the contact between the fibroblast cell and the CA1 surface (60 min and 120 min) led to pronounced increase of the adhesion force magnitude and variation. Figure 4 shows typical plots of force vs separation distance for the retraction of the fibroblast probe after it has been in contact with the CA1 surface for 10 min and 60 min, respectively. It may be seen that the f/d curves are qualitatively and quantitatively different. After 10-min contact between the cell and CA1 surface, detachment occurred over a distance of 0.1 μm. In contrast, detachment of the cell from the surface after 60-min contact occurred over about 0.5 μm and was substantially greater in

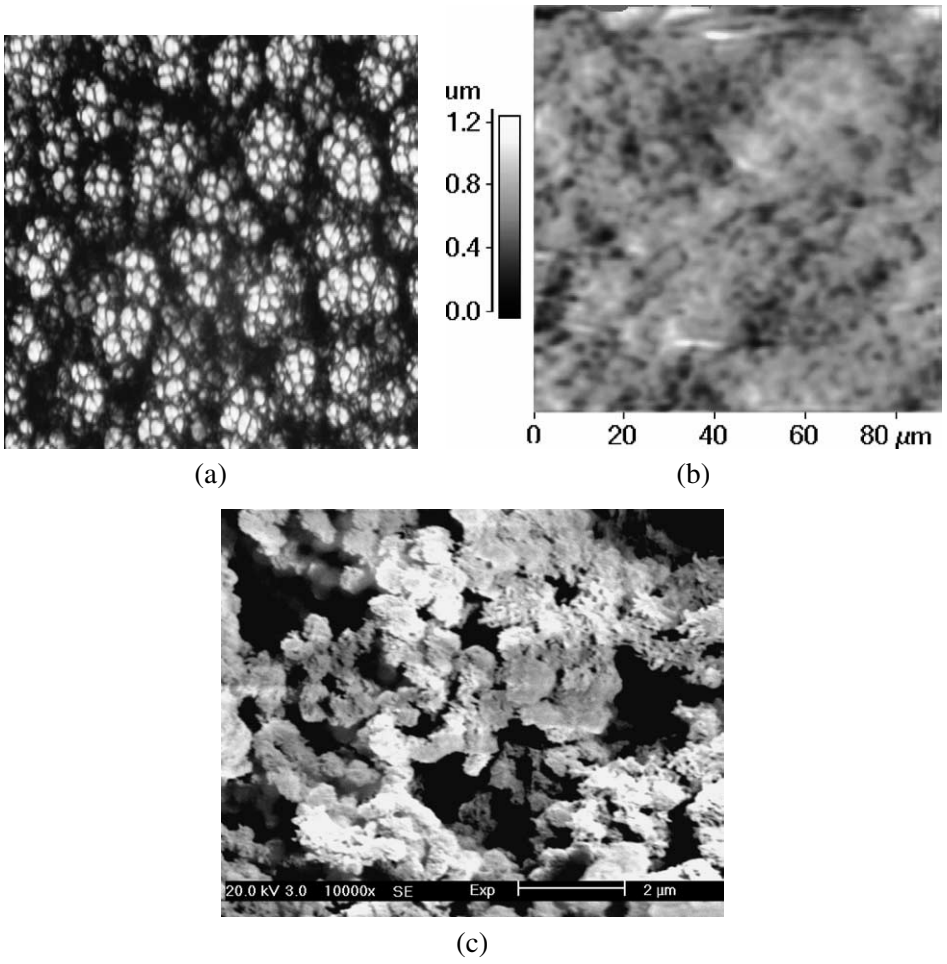

Fig. 3. (a) Optical image of the surface of CA1 scaffold; (b) AFM image of the polymeric strut surface of CA1 scaffold; (c) SEM image of internal pore wall of CA1 scaffold.

Table 2
Time-dependant initial cell/material adhesion quantified by AFM

Material	Contact duration (min)	Adhesion force (nN)
Control surface	0	26
(chamber glass slide)	10	40
PLGA3	0	3.2
	10	3.9
CA1	0	0.3
	10	1.5

magnitude than that after the short contact. The shape of the adhesion curve after long contact compared to the sharp shape after short contact indicated multiple binding of the fibroblast to the surface and a certain degree of cell stretching. Similar behavior was observed with other biological cells in contact with polymer surfaces [13].

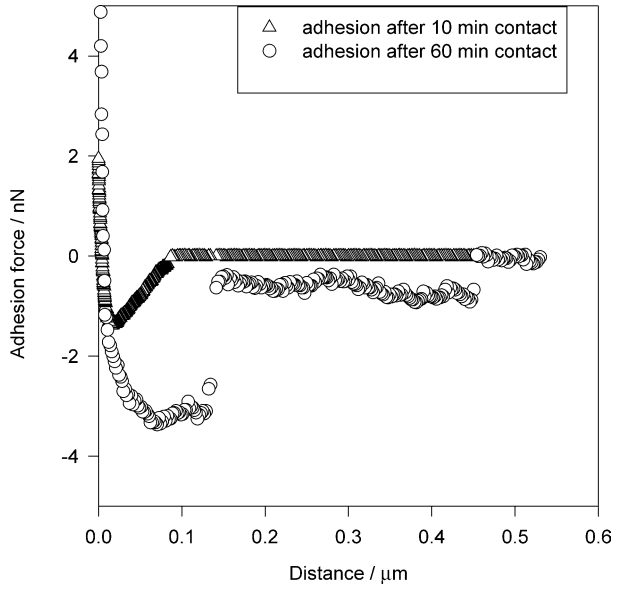

Fig. 4. AFM Force/distance retraction curves for a fibroblast probe and CA1 surface.

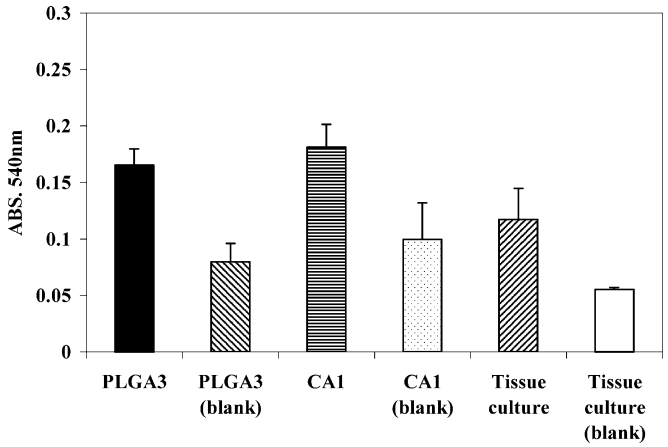

Fig. 5. HCA2 fibroblasts proliferation on the PLGA3 and CA1 scaffolds and in the absence of materials (tissue culture). Assessment of proliferation was undertaken at 72 hours using the MTT dye reduction assay. 'Blank' refers to the absence of cells. Values represent the mean ($n = 2$) $\pm$ sem. *$p < 0.05$, **$p < 0.01$.

3.3. The effect of scaffolds on cellular proliferation

Fibroblasts adhered to and proliferated on both PLGA3 and CA1 scaffolds (Fig. 5). As a control, MTT analysis was also undertaken on the materials in the absence of the cells. Both PLGA3 ($p < 0.01$) and CA1 ($p < 0.05$) stimulated fibroblast proliferation compared to their respective 'blank' controls. This was also true when cells were cultured in the absence of any materials (tissue culture; $p < 0.05$). Importantly however, compared to the absence of any materials proliferation was increased when the cells were cultured on either PLGA3 ($p < 0.05$) or CA1 ($p < 0.05$). Neither of the biomaterials demonstrated any cytotoxic potential.

4. Discussion

Instantaneous demixing process generates porous structure [14]. This accounts for the formation of porous structure of CA/DMF/water and PLGA/dioxane/ethanol systems. In contrast, the evaporation of solvent chloroform increased polymer concentration uniformly in the outermost region, leading to the dense structure of PN scaffolds. As the pore formation is governed by nucleus generation and growth, the number of nuclei and their chance of growth, therefore determine surface porosity and pore size. By adding solvent dioxane into ethanol as a nonsolvent mixture, the driving force for the exchange between nonsolvent bath and solvent is decreased. This facilitated the nucleus growth, resulting in larger pores for PLGA2 than PLGA1. In the case of formation of CA scaffolds, the evaporation of volatile solvent acetone left behind a quantity of DMF in the wet film. As DMF is a weak non-solvent for CA, the first phase separation may occur, initiating the formation of the macroporous network. By subsequent immersion into water bath, a second phase separation between the CA/acetone/water interfaces occurred, forming a porous structure of the polymeric struts. Polymeric additives PVP is a biocompatible material and has been extensively applied to increase membrane permeability and hydrophilicity [15]. It is believed that the significant increase in porosity by addition of a small amount of PVP, is due to its capability to decrease the stability of the system and enhance demixing processes. As high porosity is required to provide adequate space for cell ingrowth, this biocompatible material has potential for applications in tissue engineering. The ability of scaffolds to swell has been omitted in many studies. The high water uptake capability of both PLGA and CA scaffolds indicated that swelling should be considered in characterisation of porous scaffolds. The higher hydration degree of CA1 scaffolds is partly due to its big pore size and partly due to its high content of hydroxyl group (–OH). With such high hydration capability, the scaffolds were considered to have high surface/volume ratio and the cells can attach and grow in a three-dimensional way.

The initial adhesion of different types of cells onto various materials depends mainly on polymer surface characteristics like wettability [16], surface charge [17] and topography [18]. The initial overall cell adhesion on both scaffolds is low which was probably due to the electrostatic repulsion between negatively charged fibroblast and materials. The electrical attraction interactions between the cell and the positively charged control surface resulted in adhesion of magnitude 10–20 times greater than the adhesion measured for the biomaterials (Table 2). The higher initial cell adhesion on PLGA3 scaffold is due partly to the greater surface roughness of the material (Table 1) and partly to it's lower hydrophilicity (estimated from hydration data). The initial lowest cell attachment to CA1 surface may be primarily due to its chemical structure. Partially acetylated from cellulose (a kind of polysaccharide), cellulose acetate (CA-394-60S) still has 4% hydroxyl group (–OH) on its saccharide units. It was demonstrated that surfaces modified with a monolayer of polyethylene glycol (EG)n OH chains ($n = 6$) have the best resistance towards proteins adhesion [19,20]. An extensive survey of structures that resist the adsorption of proteins revealed that a modified sugar structure also demonstrates high resistance to protein adsorption [20]. The mechanism of resistance to adsorption of proteins remains a problem to be solved, although it is believed that the interaction of functional group, such as –OH, on the surface with water is a key component of the problem [21]. CA1 has substantially bigger pores than PLGA3 (Table 1) and control non-porous surface, which results in larger contact area with the fibroblast. In this way CA1 scaffold facilitates cells to enter inside the pores with time and interact with the inner part of the pores. It is an example of how the porous material morphology influences the cell/material attachment. The initial 10-min contact between the cell and material reflects the physical nature of the attachment when the fibroblast has a rounded shape (after trypsinization) and has yet to initiate spreading through

the production of lamellipodia. This initial cell/material adhesion is controlled mostly by the physical and chemical properties of cells and materials. When the cell was in contact with the CA1 material for a longer time (60–120 min) it began to spread on the surface through extension of lamellipodia and pseudopodia, which is known to coincide with the production and adsorption of new matrix proteins [22]. This cell spreading on the materials was directly quantified through the measured increase in the adhesion magnitude and through the multiple binding with the surface (Fig. 4). Importantly, significant cellular proliferation was found for both biomaterials compared with their controls even though they both demonstrated lower initial adhesion properties than the control. The MTT assay demonstrated increased proliferation for both the CA1 and PLGA scaffolds in comparison with the tissue culture (non-material) control (Fig. 5). However, no difference in proliferation was observed between CA1 and PGLA3 despite the initial attachment to CA1 being lower. It must be remembered however, that the proliferation data is obtained 3 days after initial attachment of the cells to the materials and hence the initial differences in adhesion may be overcome as the cells spread and begin to actively proliferate. The interesting observation is that proliferation was increased compare to control tissue culture plastic, a surface that by its very nature has been optimised for 'maximal' cellular growth. With respect to the materials it may be hypothesised that fibroblast proliferation mainly took place on the surface of PLGA3 scaffolds whereas in contrast, since the CA1 scaffold could facilitate cellular migration into the pores, proliferation may actually be taking place within the material. This awaits further elucidation but migration into and proliferation within a biomaterial are obviously highly desirable characteristics in any potential tissue engineering construct that is to have an application in the control of wound repair.

Acknowledgements

This work was funded by the UK Engineering and Physical Sciences Research Council. The authors would like to thank Professor David Kipling for the use of the immortalised HCA2 fibroblasts.

References

[1] D.W. Hutmacher, Scaffolds in tissue engineering bone and cartilage, *Biomaterials* **21** (2000), 2529–2534.
[2] P.X. Ma and R. Zhang, Synthetic nano-scale fibrous extracellular matrix, *J. Biomed. Mater. Res*. **46** (1999), 60–72.
[3] H.G. Hansma and J.H. Hoh, Biomolecular imaging with atomic force microscope, *Annu. Rev. Biophys. Biomol. Struct*. **23** (1994), 115–139.
[4] F. Braet, R. Zanger, C. Seynaeve, M. Baekeland and E. Wisse, A comparative AFM study on living skin fibroblasts and liver endothelial cells, *J. Electron Microscopy* **50**(4) (2001), 283–290.
[5] W. Haberle, J.K.H. Horber, F. Ohnesorge, D.P.E. Smith and G. Binnig, Insitu investigations of single living cells infected by viruses, *Ultramicroscopy* **42–44** (1992), 1161–1167.
[6] W.R. Bowen, T.A. Doneva and H.B. Yin, Atomic force microscopy studies of membrane–solute interactions (fouling) *Desalination* **146** (2002), 97–102.
[7] W.R. Bowen and T.A. Doneva, Atomic force microscopy of membranes, in: *Encyclopedia of Surface & Colloid Science*, Marcel Dekker, Inc., 2002, pp. 664–681.
[8] D.F. Williams, in: *Medical, Dental Materials, J. Mater. Sci. Techol-a Comprehensive Treatment*, R.W. Cahn, P. Haasen and E. Kramer, eds, VCH, Weinheim, New York, Basel, Cambridge, 1992, pp. 1–27.
[9] N. Shanmugasundaram, P. Ravichandran, P.N. Reddy, N. Ramamurty, S. Pal and K. Rao, Collagen–chitosan polymeric scaffolds for the in vitro culture of human epidermoid carcinoma cells, *Biomaterials* **22** (2001), 1943–1951.
[10] C. Liao, C. Chen, J. Chen, S. Chiang, J. Lin and K. Chang, Fabrication of porous biodegradable polymer scaffolds using a solvent merging/particulate leaching method, *J. Biomed. Mater. Res.* **59** (2002), 676–681.
[11] A.A. Ignatius and L.E. Claes, In vitro biocompatibility of bioresorbable polymers: poly(L, DL-lactide) and poly(L-lactide-co-glycolide), *Biomaterials* **17** (1996), 831–839.

[12] F.S. Wyllie, C.J. Jones, J.W. Skinner, M.F. Haughton, C. Wallis, D. Wynford-Thomas, R.G. Faragher and D. Kipling, Telomerase prevents the accelerated cell ageing of Werner syndrome fibroblasts, *Nat. Genet.* **24** (2000), 16–17.
[13] W.R. Bowen, N. Hilal, R.W. Lovitt and C.J. Wright, Direct measurement of the force of adhesion of a single cell using an atomic force microscope, *J. Colloid and Surfaces A* **136** (1998), 231–234.
[14] R.E. Kesting, The four tiers of structure in integrally skinned phase inversion membranes and their relevance to the various separation regimes, *J. Appl. Polym. Sci.* **41** (1990), 2739–2752.
[15] M. Han and S. Nam, Thermodynamic and rheological variation in polysulfone solution by PVP and its effect in preparation of phase inversion membrane, *J. Membr. Sci.* **202** (2002), 55–61.
[16] T.G. van Kooten, J.M. Schakenraad, H.C. van der Mei and H.J. Busscher, Influence of substratum wettability on the strength adhesion of human fibroblasts, *Biomaterials* **13** (1993), 897–904.
[17] S. Hattori, J.D. Andrade, J.B. Hibbs, D.E. Gregonis and R.N. King, Fibroblast cell proliferation on charged hydroxyethyl methacrylate copolymers, *J. Colloid Interface Sci.* **103** (1985), 72–78.
[18] P. van der Valk, A.W.J van Pelt, H.J. Busscher, H.P. de Jung, Ch.R.H. Wildevnur and J. Arends, Interaction of fibroblast and polymer surfaces: relationship between surface free energy and fibroblast speading, *J. Biomed. Mater. Res.* **17** (1983), 807–817.
[19] K.L. Prime and G.M. Whitesides, Adsorption of proteins onto surfaces containing end-attached oligo(ethylene oxide) – a model system using self-assembled monolayers, *J. Am. Chem. Soc.* **115** (1993), 10714–10721.
[20] E. Ostuni, R.G. Chapman, R.E. Holmlin, S. Takayama and G.M. Whitesides, A survey of structure–property relationships of surfaces that resist the adsorption of protein, *Langmuir* **17** (2001), 5605–5620.
[21] A.J. Pertsin and M. Grunze, Computer simulation of water near the surface of oligo(ethylene glycol)-terminated alkanethiol self-assembled monolayers, *Langmuir* **16** (2000) 8829–8841.
[22] P. Stephens and D.W. Thomas, The cellular proliferative phase of wound healing, *J. Wound Care* **11** (2002), 253–261.